Clinical Chemistry 55:9
1680–1685 (2009)

Copy-Number Variation Genotyping of *GSTT1* and *GSTM1* Gene Deletions by Real-Time PCR

Matthew J. Rose-Zerilli,[1,2*] Sheila J. Barton,[3] A. John Henderson,[4] Seif O. Shaheen,[5] and John W. Holloway[1,2]

BACKGROUND: Structural variation in the human genome is increasingly recognized as being highly prevalent and having relevance to common human diseases. Array-based comparative genome-hybridization technology can be used to determine copy-number variation (CNV) across entire genomes, and quantitative PCR (qPCR) can be used to validate de novo variation or assays of common CNV in disease-association studies. Analysis of large qPCR data sets can be complicated and time-consuming, however.

METHODS: We describe qPCR assays for *GSTM1* (glutathione *S*-transferase mu 1) and *GSTT1* (glutathione *S*-transferase theta 1) gene deletions that can genotype up to 192 samples in duplicate 5-μL reaction volumes in <2 h on the ABI Prism 7900HT Sequence Detection System. To streamline data handling and analysis of these CNVs by qPCR, we developed a novel interactive, macro-driven Microsoft Excel® spreadsheet. As proof of principle, we used our software to analyze CNV data for 1478 DNA samples from a family-based cohort.

RESULTS: With only 8 ng of DNA template, we assigned CNV genotypes (i.e., 2, 1, or 0 copies) to either 96% (*GSTM1*) or 91% (*GSTT1*) of all DNA samples in a single round of PCR amplification. Genotyping accuracy, as ascertained by familial inheritance, was >99.5%, and independent genotype assignments with replicate real-time PCR runs were 100% concordant.

CONCLUSIONS: The genotyping assay for *GSTM1* and *GSTT1* gene deletion is suitable for large genetic epidemiologic studies and is a highly effective analysis system that is readily adaptable to analysis of other CNVs.

The advent of microarray-based comparative genomic-hybridization technologies and whole-genome sequencing has revealed unexpectedly heterogeneous structural variation (deletions, duplications, inversions, and translocations) in the human genome *(1–3)*. These variations may have a greater effect on disease susceptibility than previously thought; therefore, it is important for any genetic study to consider the presence of structural variation in the region of interest and to have suitable technologies for detecting them *(4)*. Current technologies such as microarray-based comparative genomic hybridization and multiplex ligation-dependent probe amplification facilitate the detection of structural variation across the genome and at smaller chromosomal regions, respectively *(5, 6)*. Glutathione *S*-transferases (GSTs)[6] (EC 2.5.1.18) are phase II detoxification enzymes found free in the cytosol. These enzymes catalyze the conjugation of glutathione to many electrophilic substrates (including free radicals, xenobiotics, and physiological metabolites), producing stable and more soluble compounds that can then be excreted or compartmentalized by phase III enzymes *(7)*. The families of genes that encode GSTs are highly polymorphic in the human population *(8)*. Complete deletion of the *GSTM1*[7] (glutathione *S*-transferase mu 1) and *GSTT1* (glutathione *S*-transferase theta 1) genes occurs in approximately 50% and 20% of Caucasians, respectively. Copy-number variation (CNV) has a dosage effect on the concentrations of the GSTM1 (MIM 138350) and GSTT1 (MIM 600436) proteins that affects an individual's ability to detoxify compounds efficiently and provide protection from oxidative stress *(9, 10)*.

Polymorphisms for GST gene deletion have consequences for the detoxification of xenobiotics *(11)*. Single or combined deletions in GST-encoding genes

[1] Respiratory Genetics Group, Human Genetics, [2] Infection, Inflammation and Immunity, and [3] Public Health Sciences and Medical Statistics, Community Clinical Sciences Divisions, School of Medicine, University of Southampton, Southampton, UK; [4] Department of Community-Based Medicine, University of Bristol, Bristol, UK; [5] The National Heart and Lung Institute, Imperial College London, London, UK.

* Address correspondence to this author at: Respiratory Genetics Group, Human Genetics Division, University of Southampton, Duthie Bldg. (MP 808), Southampton General Hospital, Tremona Rd., Southampton SO16 6YD, UK. Fax +02380-794264; e-mail mjrz@soton.ac.uk.

Received February 10, 2009; accepted June 23, 2009.
Previously published online at DOI: 10.1373/clinchem.2008.120105

[6] Nonstandard abbreviations: GST, glutathione *S*-transferase; CNV, copy-number variation; ECACC, European Collection of Cell Cultures; FBAT, family-based association test; Cq, quantification cycle; qPCR, quantitative PCR.

[7] Human genes: *GSTM1*, glutathione *S*-transferase mu 1; *GSTT1*, glutathione *S*-transferase theta 1; *ALB*, albumin.

increase the susceptibility to lung cancer in smokers *(12)* and in nonsmokers exposed to household environmental tobacco smoke *(13)*. There is also an increased risk of cardiovascular disease in smokers who have a GST deficiency *(14)*. Polymorphisms for GST-encoding gene deletions and environmental tobacco smoke contribute to the development of childhood asthma *(15)* and may make asthmatic children more susceptible to the deleterious effects of ozone *(16)*.

Gross deletions in *GSTT1* and *GSTM1* genes are created by separate equal or unequal recombination events involving crossing-over between 2 highly homologous repeat regions that flank each gene *(9, 10)*. These separate recombination events produce deletion-junction regions of up to several kilobases that have very high homology (>98%) to the flanking repeat regions. This phenomenon severely restricts the design of unique primer sequences for use in standard PCR methods to identify the presence of a deletion. Sprenger et al. described a multiplex PCR method that uses unique priming sites in the *GSTT1* deletion junction *(9)*. This method appears to have limited suitability for use in large genetics studies because 2 steps, PCR amplification followed by agarose gel electrophoresis, are required to visualize the 1.46-kb deletion junction and the 466-bp gene-specific PCR products. Furthermore, unbiased coamplification of products of different sizes can be problematic, especially when the quality of the DNA is variable, because the product with the higher PCR efficiency may be preferentially amplified *(17)*.

Brasch-Andersen et al. showed that it is possible to use the increased sensitivity of real-time PCR assays to provide dosage data for the *GSTT1* and *GSTM1* genes *(18)*. This method can distinguish between individuals with 2, 1, or 0 copies of a gene. Because *GSTT1* or *GSTM1* CNV correlates with altered enzyme activity *(9, 19)*, analysis in a dose-dependent manner would best describe any association with disease outcome.

We developed new real-time PCR assays that use minor groove–binding hydrolysis probe technology on the 384-well ABI Prism 7900HT Sequence Detection System (Applied Biosystems) for higher sample throughput, and we used a novel interactive macro-driven Microsoft Excel® spreadsheet for analyzing the CNV data.

Materials and Methods

QUANTITATIVE PCR DESIGN AND VALIDATION

We used Primer Express v2.0 software (Applied Biosystems) to design novel minor groove–binding hydrolysis probe assays for target genes *GSTT1* and *GSTM1* and for reference gene *ALB* (albumin). We subsequently conducted a BLAST search (http://www.blast.ncbi.nlm.nih.gov) to evaluate the specificity of these assays. We performed PCR reactions with asymmetric concentrations of primers (0.3–0.9 μmol/L) and probe titrations (200–50 nmol/L) to lower the detection limit and to increase the cost-effectiveness of the assays, respectively. Triplicate wells of simplex (*GSTT1*, *GSTM1*, or *ALB*) and multiplex (i.e., *GSTT1* plus *ALB* or *GSTM1* plus *ALB*) reactions containing a series of 2-fold dilutions of pooled DNA samples (20–0.156 ng/reaction) from the European Collection of Cell Cultures (ECACC) were used to determine the PCR efficiencies of each assay. We performed a melting-curve analysis of the PCR to assess the specificity of the primers. Each 10-μL reaction with SYBR Green I contained 5 mmol/L $MgCl_2$, 0.2 mmol/L of each deoxynucleoside triphosphate, 30 g/L SYBR Green I (dissolved in DMSO), 0.25 U of GoldStar *Taq* DNA polymerase (Eurogentec), 10 ng of pooled control DNA template, and primers to the final concentrations detailed in Table 1 of the Data Supplement that accompanies the online version of this article at http://www.clinchem.org/content/vol55/issue9. To evaluate genotyping accuracy, we used replicate sample wells and conducted transmission disequilibrium tests with family-based association test (FBAT) v1.4 *(20)* as an inheritance check for the family-based cohort.

DNA TEMPLATES

ECACC Human Random Control DNA samples (HRC-1) (http://www.hpacultures.org.uk/collections/ecacc.jsp) were used to optimize reaction conditions, to determine the stability of reaction plate storage, and to validate subsequent experiments as positive controls. Details of the ECACC HRC-1 DNA samples used as controls are described in the user manual for CNV analysis in the online Data Supplement. We conducted *GSTT1* and *GSTM1* CNV experiments with 1478 DNA samples previously collected for an asthma study of sibling pairs from 341 affected Caucasian families in the UK *(21)*. Samples were obtained with informed consent after ethics approval from the Southampton and South West Hampshire Local Research Ethics Committee and the Portsmouth and South East Hampshire Local Research Ethics Committee.

PROTOCOL

We transferred 2 μL of 1-ng/μL genomic DNA in duplicate to a 384-well plate. Each plate also contained 3 positive controls and a minimum of 4 negative controls (water). Before adding the reaction mixture, we dried the DNA for 10 min at 80 °C on a PCR thermal cycler.

We used 5 μL for each multiplex assay, and each well contained the following: 2.5 μL of 2× Precision-R MasterMix (PrimerDesign), which contained 5 mmol/L $MgCl_2$, 200 μmol/L of each deoxynucleoside triphosphate, 0.025 U/μL *Taq* polymerase, and 6-carboxy-X-rhodamine reference dye; the necessary volume of

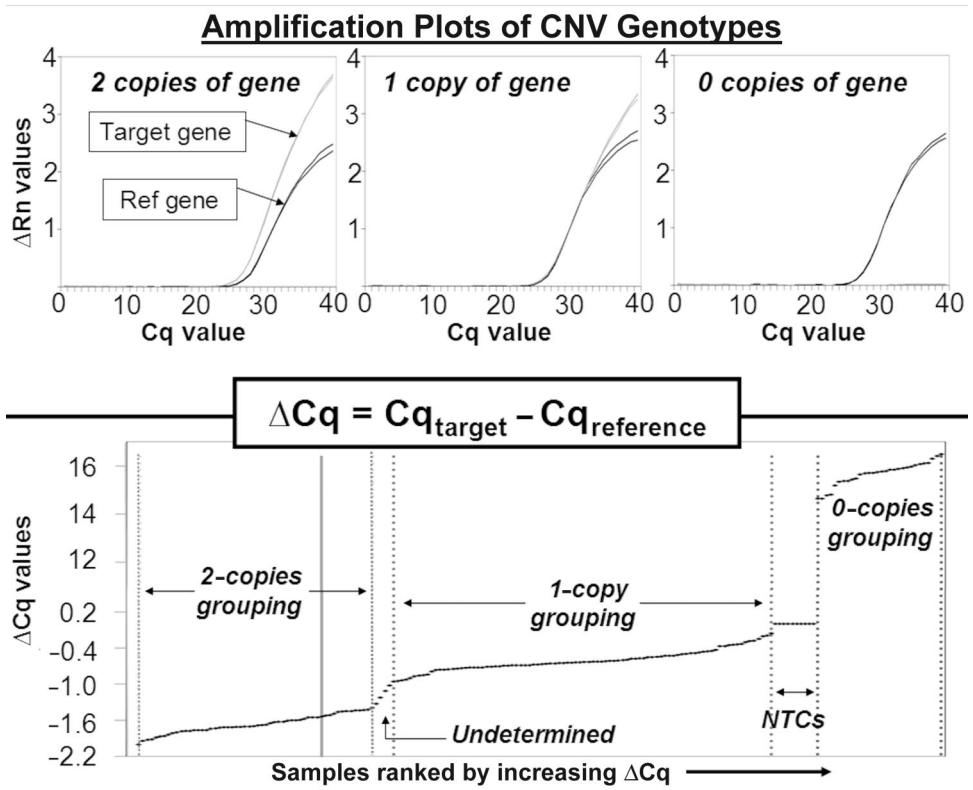

Fig. 1. CNV analysis spreadsheet.

Real-time PCR data are imported into the analysis spreadsheet, and the macro calculates the difference between the target and reference Cq values with the indicated formula. ΔCq values are displayed in a ranked scatter graph (bottom chart), allowing assignment of CNV-genotype groupings by moving the vertical dotted lines. The solid vertical line highlights any desired sample and displays the PCR curves; this feature allows determination of the validity of any genotype assignment within the grouping. The top 3 graphs display plots of PCR curves for each of the 3 possible CNV genotypes. ΔRn, reporter signal normalized to ROX; Ref, reference; NTCs, no-template controls.

primer/probe mix; and PCR-grade water to volume. Table 1 in the online Data Supplement lists primer and probe sequences and reagent concentrations in the reactions. All PCR reaction mixes were prepared in bulk with 10% extra volume for pipetting and were transferred to the 384-well plate with an electronic multichannel pipettor. Primer/probe mixes were also prepared in advance to reduce the interassay imprecision attributable to setting up each PCR reaction mix.

The plates were heat-sealed (Thermo-Sealer; ABgene) to stop any evaporation from occurring during the DNA-rehydration step (30 min at 4 °C protected from light, with periodic mixing) and during thermal cycling. PCR amplification and collection of real-time fluorescence data were performed on the ABI Prism 7900HT Sequence Detection System. The thermal profile consisted of incubation at 95 °C for 10 min followed by 40 cycles of 95 °C for 15 s and 60 °C for 60 s without 9600-emulated temperature ramping. Fluorescence data were collected during the 60 °C annealing/extension cycles, and quantification cycle (Cq) values were calculated with the automatic Cq-analysis settings on an absolute quantification run (SDS Plate Utility v2.1; Applied Biosystems).

CNV ANALYSIS SPREADSHEET

We designed a macro-based Microsoft Excel spreadsheet to analyze real-time PCR data for gene dosage (Fig. 1). The results (Cq values) and files of clipped data (normalized fluorescence values from the reporter dyes at the end of each extension phase) generated by the SDS v2.1 software for each plate run can be imported into the spreadsheet. Each duplicate data point is visualized in a ranked *xy* scatter graph (ΔCq value vs samples ranked by increasing ΔCq). The ΔCq value ($\Delta Cq = Cq_{target} - Cq_{reference}$) for each duplicate can be

compared directly with the plots of real-time amplification curves generated by each grouping of sample wells. The interactive sliding windows allow semiautomated assignment of genotype groups and outliers on the basis of the grouping of ΔCq values on the ranked *xy* scatter graph. Importantly, interrogation of the plots of real-time amplification curves permits rapid determination of the validity of any genotype call and allows manual correction. The spreadsheet automatically calculates CNV and frequencies of a gene present or absent, deviation from the Hardy–Weinberg equilibrium, and several QC parameters (i.e., mean ΔCq value and SD of each CNV group). The interactive and color-coded 384- and 96-well arrays of the plate layout generated by the macro also allows postanalysis visualization of the well position for any genotype call, water control, or reaction failure. This utility allows monitoring for any problematic samples or experimental controls. It also identifies any possible effects of the plate edges on data quality. Finally, the macro exports all analyzed data to a new sheet in the spreadsheet in a database-compatible format (Microsoft Access®). The CNV-analysis spreadsheet is available in the online Data Supplement.

CALCULATIONS OF THE HARDY–WEINBERG EQUILIBRIUM

These calculations were performed on the parental genotypes with the online version of the Definetti program (http://ihg.gsf.de/cgi-bin/hw/hwa1.pl). A Pearson χ^2 P value <0.05 was considered to indicate significant deviation of the genotype frequency from the Hardy–Weinberg equilibrium.

Results

ASSAY OPTIMIZATION

The detection limits of the quantitative PCR (qPCR) assays were substantially improved with the use of asymmetric concentrations of primers (see Table 1 in the online Data Supplement). These conditions reduced Cq values by up to 1.38 Cq. Titrations of the probe concentration revealed that a final probe concentration of 150 nmol/L for each assay could be used without decreasing the signal strength (lower signal-to-noise ratio) or the detection limit (increase in Cq value). An analysis of the SYBR Green I melting curve revealed single melting peaks for all assays (see Fig. 1 in the online Data Supplement).

Under multiplex conditions and the optimized asymmetric primer concentrations and probe concentrations described above, the calibration curves (see Fig. 2 in the online Data Supplement) demonstrated that the multiplex amplification reactions were linear over the entire range of DNA template concentrations (20–0.156 ng); all values for PCR reaction efficiency ($E = 10^{1/s}$, where s is the slope of the calibration curve) were between 1.95 and 1.99, values close to the theoretical maximum value (i.e., $E = 2.0$, in which 1 Cq is equivalent to a doubling of the PCR product with each PCR cycle). The interassay variation in PCR efficiency was <1% in both multiplex reactions (E_{GSTM1} and E_{ALB}, 0.65%; E_{GSTT1} and E_{ALB}, 0.01%), confirming that both PCR products in the multiplex were amplifying at nearly the same rate.

Table 1. ΔCq values for GST CNV genotypes.[a]

Gene	CNV genotype	Samples, n	Mean ΔCq	ΔCq SD	Mean difference: $\Delta Cq_{2\ copies} - \Delta Cq_{1\ copy}$
GSTM1	2	5	−1.25	0.09	1.03
	1	64	−0.22	0.16	
	0	112	12.90	1.14	
GSTT1	2	54	−1.67	0.15	1.06
	1	90	0.61	0.18	
	0	30	15.66	0.49	

[a] Mean ΔCq values for each genotype group for 176 DNA samples.

The SD for the mean ΔCq ($\Delta Cq = Cq_{target} - Cq_{reference}$) determined at each DNA dilution along the calibration curve was used to estimate the experimental variation in the ΔCq value used to determine the copy number for the gene of interest. Over the range of DNA dilutions (20–0.156 ng), the mean (SD) ΔCq was −0.72 (0.1) for the *GSTM1* assay and −0.54 (0.08) for the *GSTT1* assay.

The initial genotyping results for the 2 genes obtained for 176 DNA samples (Table 1) demonstrated that the sensitivity of the qPCR assay was sufficient so that ΔCq values could be used to distinguish a change in gene copy number. The mean difference in ΔCq between samples assigned a 2-copies or 1-copy genotype was 1.03 for *GSTM1* and 1.06 for *GSTT1*. These values were very close to the theoretical 1 Cq value for a doubling in concentration (i.e., 1 extra copy of the gene). In practice, this value varied slightly between plate runs (0.85–1.20), although this variation did not affect genotyping accuracy because the data from each plate were analyzed independently in the analysis spreadsheet.

GENOTYPING RESULTS

Genotyping accuracies for the *GSTM1* (99.9%) and *GSTT1* (99.5%) assays were determined by dividing the number for non-Mendelian inheritances detected with the FBAT program by the number of child genotypes (n = 770 for *GSTM1*; n = 735 for *GSTT1*). All of the results indicating non-Mendelian inheritance (n = 1

Table 2. Genotype frequencies.[a]

Group	Gene	CNV frequency, n (%) 2 Copies	1 Copy	0 Copies	HWE *P*
Entire cohort	*GSTT1*	415 (31)	690 (51)	247 (18)	NA
	GSTM1	98 (7)	534 (38)	786 (55)	NA
Parents only	*GSTT1*	193 (31)	321 (52)	103 (17)	0.117
	GSTM1	42 (6)	250 (39)	356 (55)	0.831

[a] Calculations of the Hardy–Weinberg equilibrium (HWE) were not performed on the full family cohort because the individuals are related; the parents' frequencies were analyzed separately as a surrogate of that of the general population and found to be in HWE. NA, not applicable.

for *GSTM1*; n = 4 for *GSTT1*) were due to child "2 copies" genotype calls when the parental genotype combination permitted only 0- or 1-copy offspring. To test the interassay reproducibility of genotype assignments, we re-genotyped 92 DNA samples for both CNVs in a separate qPCR run; comparison of the 2 independent genotype calls demonstrated 100% concordance. Table 2 shows the full cohort and parent genotype frequencies for both gene CNVs and a lack of statistical significance in Pearson tests for deviation from the Hardy–Weinberg equilibrium. The rates for undetermined CNV calls (i.e., 2, 1, and 0 copies) were 4% for *GSTM1* and 9% for *GSTT1*, and 2% and 3%, respectively, for the gene absent/present call.

ASSAY PLATE STABILITY

Testing performed at the 24-h, 48-h, and 72-h time points with the ECACC HRC-1 DNA panel showed that sealed reaction plates could be stored protected from light at room temperature for 24 h before the real-time PCR run without any degradation in data quality (data not shown).

Discussion

This new methodology enhances the study of gene CNV in the large sample sizes required in genetic-association studies. This study is not the first application of real-time PCR to assay *GSTM1* and *GSTT1* CNV; several other protocols have been described in the literature *(18, 22)*. These methods are not effective, however, for processing the large sample sizes required in genetic-association studies, because the low sample density on reaction plates caused by the use of triplicate wells and larger reaction volumes (10 μL) result in a high genotyping cost per sample. With our method, 96 samples can be genotyped for 2 CNVs in duplicate wells on a single reaction plate (or 192 samples for 1 CNV) in <2 hours with a proportional 66% savings in the costs for 2× Precision-R MasterMix (5 μL vs 15 μL), primers, and probe. The small amount of DNA template used in the assay conserves DNA template (4 ng DNA per CNV). Diluting the template also dilutes any potential PCR inhibitors present in the sample, and drying the template reduces sample cross-contamination. We determined 2 ng DNA to be optimum in our genotyping experiments because this quantity falls in the central part of the range of calibrator dilutions where Cq values have a direct relationship to the log of the DNA template concentration, thus providing accurate quantification. Minor groove–binding hydrolysis probes were used because they permitted smaller reaction volumes than required with standard hydrolysis probes without compromising the assay's detection limit or reproducibility *(23)*. The calibration curves demonstrate that the multiplex PCR reactions are highly efficient ($E \geq 1.95$) and amplify at nearly the same rate with a large dynamic range. The calibration curves cover a DNA template concentration range of 7 "orders of magnitude" (i.e., 2^0–2^{-7}: 20–0.156 ng DNA per PCR reaction).

The combination of assay optimization and use of a novel analysis spreadsheet enabled these assays to report 97%–98% of the individuals in our family cohorts with gene present/absent genotype calls and 91%–96% of the individuals with full CNV genotypes (i.e., 0, 1, or 2 copies) with high accuracy (≥99.5%, as determined by evaluating inheritance in the family cohort). Success rates for calling full CNV genotypes approached those routinely achieved by standard technologies for calling genotypes for single-nucleotide polymorphisms (≥95%) *(24)*. A subsequent round of genotyping for the unassigned samples (between 6% and 9% for *GSTM1* and *GSTT1*) increases the genotyping success rate to the rates achieved with the genotyping technologies used for single-nucleotide polymorphisms while still obtaining a greater proportional savings in costs compared with previously described GST CNV protocols *(18, 22)*. The detection of a small number of non-Mendelian inheritances in our cohort of families may reflect a possible limitation of the manual sliding-window method to determine the end of the 2-copies ΔCq grouping and the start of the single-copy grouping (i.e., 1-copy individuals could be erroneously assigned to the 2-copies group). The start and end of the 2 groupings of genotypes on the ranked *xy* scatter graph are usually distinct, however, and barring any outlying data points (outliers can easily be distinguished by examining the quality of the data for real-time PCR plots for the well grouping), the FBAT-determined inheritance results could simply reflect the true genotyping error of the technique (i.e., sporadic contamination not detected by the negative controls and chance results). In support of this hypothesis, the genotypes of re-genotyped samples were 100% concordant,

and the lack of any discordant genotypes indicated that the manual sliding-window method for assigning genotype groups was sound.

The protocol described in this report has advantages over previously published methodologies *(18, 22)*, including a higher sample density per reaction plate, a smaller reaction volume, and compatibility with liquid-handling robotic platforms for DNA aliquoting, reaction plate setup, and loading of plates onto the real-time PCR machine. The analysis spreadsheet provides a complete analysis, QC, troubleshooting capabilities, and a data-handling solution to CNV genotyping on the ABI 7900HT Sequence Detection System. The macro-based Excel spreadsheet eliminates the considerable bottleneck involved in processing real-time PCR data and may be applicable to CNV genotyping of other genes from any genome.

Author Contributions: *All authors confirmed they have contributed to the intellectual content of this paper and have met the following 3 requirements: (a) significant contributions to the conception and design, acquisition of data, or analysis and interpretation of data; (b) drafting or revising the article for intellectual content; and (c) final approval of the published article.*

Authors' Disclosures of Potential Conflicts of Interest: *Upon manuscript submission, all authors completed the Disclosures of Potential Conflict of Interest form. Potential conflicts of interest:*

Employment or Leadership: None declared.
Consultant or Advisory Role: None declared.
Stock Ownership: None declared.
Honoraria: None declared.
Research Funding: M.J. Rose-Zerilli, The British Lung Foundation; Asthma, Allergy & Inflammation Research Charity; and the Infection, Inflammation and Immunity Division, School of Medicine, University of Southampton. J.W. Holloway, The Medical Research Council UK; The British Lung Foundation; Asthma UK; and the Asthma, Allergy & Inflammation Research Charity. S.O. Shaheen, Asthma UK.
Expert Testimony: None declared.

Role of Sponsor: The funding organizations played no role in the design of study, choice of enrolled patients, review and interpretation of data, or preparation or approval of manuscript.

References

1. Feuk L, Carson AR, Scherer SW. Structural variation in the human genome. Nat Rev Genet 2006; 7:85–97.
2. Levy S, Sutton G, Ng PC, Feuk L, Halpern AL, Walenz BP, et al. The diploid genome sequence of an individual human. PLoS Biol 2007;5:e254.
3. Sharp AJ, Locke DP, McGrath SD, Cheng Z, Bailey JA, Vallente RU, et al. Segmental duplications and copy-number variation in the human genome. Am J Hum Genet 2005;77:78–88.
4. Feuk L, Marshall CR, Wintle RF, Scherer SW. Structural variants: changing the landscape of chromosomes and design of disease studies. Hum Mol Genet 2006;15:R57–66.
5. Carson AR, Feuk L, Mohammed M, Scherer SW. Strategies for the detection of copy number and other structural variants in the human genome. Hum Genomics 2006;2:403–14.
6. Bunyan DJ, Eccles DM, Sillibourne J, Wilkins E, Thomas NS, Shea-Simonds J, et al. Dosage analysis of cancer predisposition genes by multiplex ligation-dependent probe amplification. Br J Cancer 2004;91:1155–9.
7. Frova C. Glutathione transferases in the genomics era: new insights and perspectives. Biomol Eng 2006;23:149–69.
8. McIlwain CC, Townsend DM, Tew KD. Glutathione *S*-transferase polymorphisms: cancer incidence and therapy. Oncogene 2006;25:1639–48.
9. Sprenger R, Schlagenhaufer R, Kerb R, Bruhn C, Brockmoller J, Roots I, Brinkmann U. Characterization of the glutathione *S*-transferase *GSTT1* deletion: discrimination of all genotypes by polymerase chain reaction indicates a trimodular genotype-phenotype correlation. Pharmacogenet 2000;10:557–65.
10. Xu S, Wang Y, Roe B, Pearson WR. Characterization of the human class Mu glutathione *S*-transferase gene cluster and the *GSTM1* deletion. J Biol Chem 1998;273:3517–27.
11. Bolt HM, Thier R. Relevance of the deletion polymorphisms of the glutathione *S*-transferases *GSTT1* and *GSTM1* in pharmacology and toxicology. Curr Drug Metab 2006;7:613–28.
12. Sorensen M, Autrup H, Tjonneland A, Overvad K, Raaschou-Nielsen O. Glutathione *S*-transferase T1 null-genotype is associated with an increased risk of lung cancer. Int J Cancer 2004;110: 219–24.
13. Wenzlaff AS, Cote ML, Bock CH, Land SJ, Schwartz AG. GSTM1, GSTT1 and GSTP1 polymorphisms, environmental tobacco smoke exposure and risk of lung cancer among never smokers: a population-based study. Carcinogenesis 2005;26:395–401.
14. Tamer L, Ercan B, Camsari A, Yildirim H, Cicek D, Sucu N, et al. Glutathione *S*-transferase gene polymorphism as a susceptibility factor in smoking-related coronary artery disease. Basic Res Cardiol 2004;99:223–9.
15. Kabesch M, Hoefler C, Carr D, Leupold W, Weiland SK, von Mutius E. Glutathione *S* transferase deficiency and passive smoking increase childhood asthma. Thorax 2004;59:569–73.
16. Romieu I, Sienra-Monge JJ, Ramirez-Aguilar M, Moreno-Macias H, Reyes-Ruiz NI, Estela del Rio-Navarro B, et al. Genetic polymorphism of *GSTM1* and antioxidant supplementation influence lung function in relation to ozone exposure in asthmatic children in Mexico City. Thorax 2004;59: 8–10.
17. Markoulatos P, Siafakas N, Moncany M. Multiplex polymerase chain reaction: a practical approach. J Clin Lab Anal 2002;16:47–51.
18. Brasch-Andersen C, Christiansen L, Tan Q, Haagerup A, Vestbo J, Kruse TA. Possible gene dosage effect of glutathione-*S*-transferases on atopic asthma: using real-time PCR for quantification of *GSTM1* and *GSTT1* gene copy numbers. Hum Mutat 2004;24:208–14.
19. McLellan RA, Oscarson M, Alexandrie AK, Seidegard J, Evans DA, Rannug A, Ingelman-Sundberg M. Characterization of a human glutathione *S*-transferase mu cluster containing a duplicated *GSTM1* gene that causes ultrarapid enzyme activity. Mol Pharmacol 1997;52:958–65.
20. Laird NM, Horvath S, Xu X. Implementing a unified approach to family-based tests of association. Genet Epidemiol 2000;19(Suppl 1):S36–42.
21. Van Eerdewegh P, Little RD, Dupuis J, Del Mastro RG, Falls K, Simon J, et al. Association of the ADAM33 gene with asthma and bronchial hyperresponsiveness. Nature 2002;418:426–30.
22. Covault J, Abreu C, Kranzler H, Oncken C. Quantitative real-time PCR for gene dosage determinations in microdeletion genotypes. Biotechniques 2003;35:594–6, 8.
23. Kutyavin IV, Afonina IA, Mills A, Gorn VV, Lukhtanov EA, Belousov ES, et al. 3′-minor groove binder-DNA probes increase sequence specificity at PCR extension temperatures. Nucleic Acids Res 2000;28:655–61.
24. Tindall EA, Speight G, Petersen DC, Padilla EJ, Hayes VM. Novel Plexor SNP genotyping technology: comparisons with TaqMan and homogenous MassEXTEND MALDI-TOF mass spectrometry. Hum Mutat 2007;28:922–7.